Mediterranean Journal of Medical Research
ISSN Online: 2789-1895
Mediterr J Med Res
doi: 10.5281/zenodo.18945545
https://mrj.org.ly

ORIGINAL RESEARCH article

Computational screening of natural small molecules as dual ATXN3 and LC3 binders for an autophagy-based strategy in spinocerebellar ataxia type 3

Shada H. Alharati [1], **Halima A. Gbaj** [2], **Mohamed A. Gbaj** [3]
Anton Hermann [4], and **Abdul M. Gbaj** [1, 5 *]

[1] Department of Chemistry and Toxins, Judicial Expertise and Research Center, Tripoli, Libya
[2] Department of Microbiology and Immunology, Faculty of Pharmacy, University of Tripoli, Tripoli, Libya
[3] Department of Chemical Engineering, Faculty of Engineering, University of Tripoli, Tripoli, Libya
[4] Department of Biosciences, University of Salzburg, Salzburg, Austria
[5] Department of Medicinal Chemistry, Faculty of Pharmacy, University of Tripoli, Tripoli, Libya
[*] Author to whom correspondence should be addressed

Received: 09-011-2025, **Accepted:** 03-03-2026, **Published online:** 10-03-2026

Copyright© 2026. This open-access article is distributed under the *Creative Commons Attribution License*, which permits unrestricted use, distribution, and reproduction in any medium, provided the original work is properly cited.

HOW TO CITE THIS
Alharati et al. Computational screening of natural small molecules as dual ATXN3 and LC3 binders for an autophagy-based strategy in spinocerebellar ataxia type 3. Mediterr J Med Res. 2026; 3(1): 94-104. [Article number: 44]. https://doi.org/10.5281/zenodo.18945545

Keywords: AutoDock vina, autophagosome docking, dual target binding, SwissADME, pharmacokinetics

Abstract: Spinocerebellar ataxia type 3 (SCA3) is an autosomal dominant neurodegenerative disorder caused by a CAG repeat expansion in the ATXN3 gene, producing a polyglutamine expanded ataxin-3 protein that misfolds, aggregates, and drives progressive neurodegeneration. Enhancing the selective autophagic clearance of mutant ATXN3 through recruitment to the autophagy adaptor LC3 on autophagosomal membranes represents a promising disease-modifying strategy. This study investigates whether natural small molecules can act as dual binders of ATXN3 and LC3, providing accessible scaffolds for an autophagy-based therapeutic approach in SCA3. The Josephin domain of human ATXN3 and human LC3 were prepared as receptor structures. Five natural ligands, quercetin, kaempferol, luteolin, rutin, and trehalose, were subjected to Vina-based molecular docking. For each ligand-target pair, the lowest energy pose was selected and analyzed for predicted binding free energies (ΔG, kcal/mol), hydrogen bond networks, and hydrophobic contacts. Pharmacokinetic properties were evaluated using SwissADME to assess drug likeness and oral bioavailability. Quercetin, kaempferol, and luteolin showed strong and balanced predicted binding to ATXN3 (-8.5 to -8.1 kcal/mol) and LC3 (-8.4 to -8.3 kcal/mol), with molecular weights 286-302 g/mol, high predicted gastrointestinal absorption, and no Lipinski violations. Rutin and trehalose bound ATXN3 weakly (-6.4 and -5.2 kcal/mol, respectively) but displayed strong ending to LC3 (-10.3 and -7.8 kcal/mol), though with poor oral drug-like properties (MW 610.52 and 342.30 g/mol, respectively, low gastrointestinal absorption and multiple Lipinski violations. Common natural flavonoids, particularly quercetin, kaempferol, and luteolin, exhibit strong dual-target binding with favorable oral drug-like properties, supporting their potential as simple scaffolds for autophagy-based therapeutic strategies in SCA3. These findings provide a clear rationale for subsequent biochemical and cellular validation of their ATTEC like mechanisms.

Introduction

Spinocerebellar ataxia type 3 (SCA3) is the most prevalent form of autosomal dominant spinocerebellar ataxia worldwide [1]. It results from an expansion of CAG repeats in the ATXN3 gene, generating a polyglutamine

expanded ataxin-3 protein that is prone to misfolding and aggregation. Aggregated ATXN3 accumulates in neuronal nuclei and cytoplasm and is associated with progressive loss of neurons in the cerebellum, brainstem, and other regions [2-6]. Clinically, patients develop gait and limb ataxia, dysarthria, oculomotor abnormalities, and a variety of pyramidal and extrapyramidal signs, with considerable phenotypic heterogeneity. Despite increasing understanding of the molecular pathology, there is no approved therapy that alters disease progression [1, 6, 7]. To summarize the main steps linking ATXN3 polyQ expansion to neurodegeneration and highlight the points where proteostasis pathways intervene, the proposed pathology cascade is outlined in **Figure 1**.

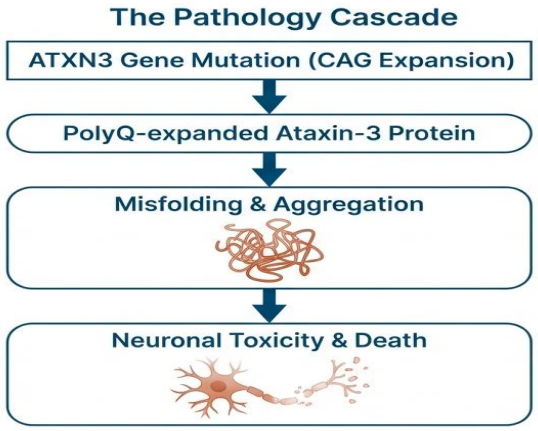

Figure 1: The pathology cascade in spinocerebellar ataxia type 3

Protein misfolding and aggregation are shared features of many neurodegenerative diseases, including other polyglutamine disorders and conditions such as Huntington's disease and certain forms of amyotrophic lateral sclerosis. The balance between protein synthesis, folding, and degradation is maintained by cellular quality control pathways, notably the ubiquitin proteasome system and autophagy. When these systems are overwhelmed or impaired, aggregation-prone proteins accumulate and exert toxic effects on neuronal function and survival [1, 4, 5, 8, 9].

Autophagy is a major degradative pathway for long-lived proteins, protein aggregates, and damaged organelles. During autophagy, cytosolic material is sequestered within a double membrane autophagosome that subsequently fuses with a lysosome, where the cargo is degraded. LC3 plays a central role in this process. The cytosolic LC3-I form is converted to a lipidated LC3-II form that stably associates with autophagosomal membranes. LC3-II interacts with autophagy receptors bearing LC3-interacting region motifs, thereby linking specific cargo to the autophagic machinery and allowing selective degradation of aggregated proteins or organelles [2, 3, 9-12]. Given the importance of LC3 in cargo recognition, small molecules that can modulate LC3 interactions are of growing interest [13, 14]. An elegant example is provided by autophagosome tethering compounds (ATTECs) [15, 16], which are designed to bind LC3 and a target protein, physically bridging them and promoting selective autophagic degradation of the target. In models of polyglutamine disorders, ATTECs have been used to reduce levels of mutant huntingtin and aggregation-prone proteins, with corresponding improvements in cellular and behavioral phenotypes [17]. These findings highlight a general strategy: Instead of stimulating autophagy globally, one can redirect the autophagy machinery toward specific toxic proteins. Parallel to these synthetic approaches, numerous natural compounds have been reported to exert neuroprotective effects and to influence autophagy.

Flavonoids such as quercetin, kaempferol, luteolin, and rutin are abundant dietary polyphenols with antioxidant anti-inflammatory signaling properties. Several studies suggest that they can modulate autophagy-related pathways in neural and non-neural cells [18-20]. Trehalose, a non-reducing disaccharide, has been shown to

enhance autophagy and to reduce the aggregation and toxicity of mutant polyglutamine proteins, including ATXN3, in experimental models [21-23]. However, it remains unclear whether these natural compounds can directly engage mutant ATXN3 and LC3 in a way that would support an ATTEC-like mechanism [24, 25]. The five selected natural ligands and their key chemical features are presented in **Table 1**.

Table 1: IUPAC name, functional group, and chemical structure of the natural ligands (quercetin, kaempferol, luteolin, rutin, and trehalose) investigated in this study for dual ATXN3-LC3 binding

Name	IUPAC Name	Main functional Groups	Chemical Structure
Quercetin	2-(3,4-Dihydroxyphenyl)-3,5,7-trihydroxychromen-4-one	Hydroxyl (-OH), Ketone (C=O), Ether	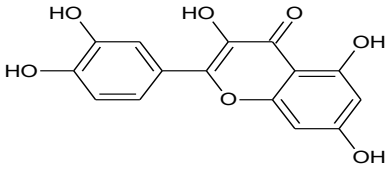
Kaempferol	3,5,7-Trihydroxy-2-(4-hydroxyphenyl)-4H-chromen-4-one	Hydroxyl (-OH), Ketone (C=O), Ether	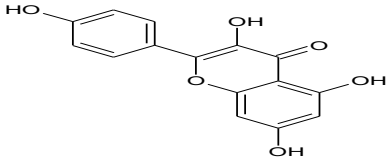
Luteolin	2-(3,4-Dihydroxyphenyl)-5,7-dihydroxychromen-4-one	Hydroxyl (-OH), Ketone (C=O), Ether	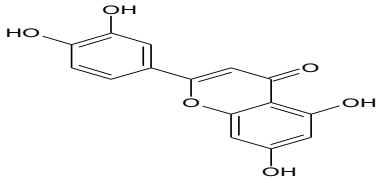
Rutin	2-(3,4-Dihydroxyphenyl)-5-hydroxy-7-[(2S,3R,4S,5S,6R)-3,4,5-trihydroxy-6-[[(2R,3R,4R,5R,6S)-3,4,5-trihydroxy-6-methyloxan-2-yl]oxymethyl]oxan-2-yl]oxychromen-4-one	Hydroxyl (-OH), Glycosidic bonds, Ketone	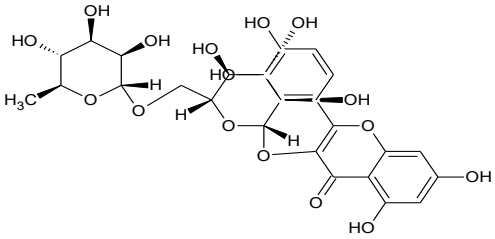
Trehalose	α-D-Glucopyranosyl α-D-glucopyranoside	Hydroxyl (-OH), Glycosidic bond (α-1,1)	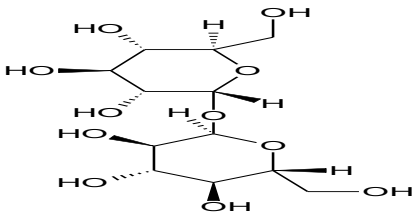

The aim of the present study was to explore, using a structure-based computational approach, whether common natural small molecules could act as dual binders of the ATXN3 Josephin domain and LC3. Four flavonoids (quercetin, kaempferol, luteolin, rutin) and trehalose were selected as ligands because of their favorable safety profiles and prior evidence of neuroprotective or autophagy-related activity [18, 19, 21, 26-28]. By docking these compounds to the ATXN3 Josephin domain and to LC3, by analyzing their binding energies and interaction patterns, and by assessing their pharmacokinetic properties, the study was sought to identify promising scaffolds that could be further developed into small molecules supporting selective autophagic clearance of mutant ATXN3. Because the central concept of this study is an ATTEC-like bridging approach between LC3 and a disease protein, the strategy is schematized in **Figure 2**.

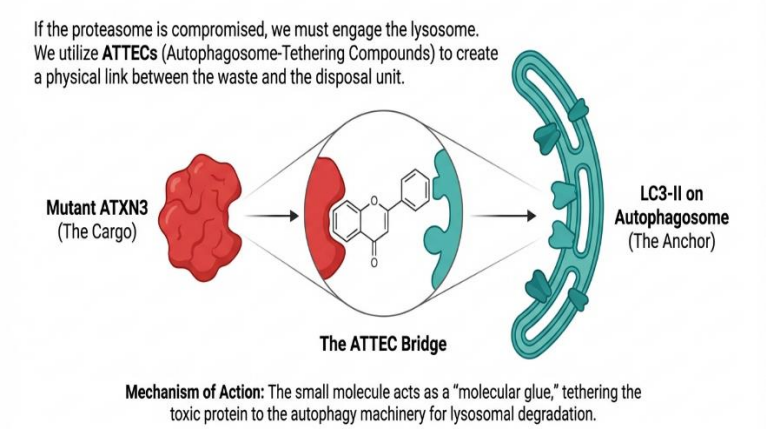

Figure 2: The ATTEC Strategy: Hijacking the autophagy pathway for selective ATXN3 clearance

Materials and methods

Target structure: The disease related target was the Josephin domain of ataxin-3. The NMR structure corresponding to residues 1-182 of human ATXN3 was used as the receptor, representing the catalytic N-terminal domain that participates in de-ubiquitinase activity and protein-protein interactions. Although the toxic poly-glutamine tract resides in the C-terminal region, the structured Josephin domain provides the most reliable template for structure-based analysis of ligand binding [29-32]. LC3 was chosen as the autophagy adaptor target [9, 24, 33]. The crystal structure of human LC3 bound to a peptide ligand [34] was obtained from the Protein Data Bank [35]. This structure reveals the hydrophobic pockets and surrounding residues responsible for recognizing LC3-interacting region motifs and has widely been used to study LC3-ligand interactions. Prior to docking, co-crystallized peptides, water molecules, and other heteroatoms were removed from the structures. Polar hydrogens were added, appropriate protonation states at physiological pH were assigned, and charges were applied using a standard preparation protocol compatible with the Vina docking engine [36]. The processed structures were saved in the required receptor format.

Ligand preparation: The ligand panel consisted of quercetin, kaempferol, luteolin, rutin, and trehalose [37-43]. For standardized depiction, 2D structure diagrams of all ligands were redrawn using ACD/ChemSketch [43] and exported in a vector format for inclusion in **Table 1**. For docking, ligand structures were obtained from public databases [37-41] and converted to 3D conformers as described below. Each ligand was subjected to geometry optimization using a standard molecular mechanic's force field. Rotatable bonds were identified, and torsional degrees of freedom were defined to allow flexible ligand sampling during docking. Ligands were saved in the appropriate input format with assigned partial charges.

Docking protocol: Molecular docking was carried out using a Vina-based workflow [36], which predicts ligand-protein binding modes and provides an approximate binding free energy (ΔG, kcal/mol) for each pose. For

ATXN3, the search space was defined around a surface cleft identified in preliminary dockings and composed primarily of residues Gly25-Gly29, Leu26, Ala27, Ala16, Ala45, and Ser114. For LC3, the grid box was centered on the canonical LC3 ligand binding pockets and neighboring grooves enriched in polar and charged residues, including Lys2046, Arg2154, Asp2233, Gln1188, Lys2140, Ser2050, Asn2048, and Gln2127. For every ligand-target pair, multiple docking runs were performed to sample alternative poses. The best pose for each complex was selected based on the lowest predicted binding energy and visual inspection for chemically reasonable interactions and absence of obvious steric clashes. Binding energies were recorded as near ΔG values in kcal/mol.

Interaction analysis: The selected poses were analyzed using molecular visualization software, including PyRx virtual screening software and BIOVIA Discovery Studio Visualizer [43, 44] for visualization and interaction analysis. Hydrogen bonds between ligand and receptor were identified using standard geometric criteria for donor-acceptor distance and angle. The number of hydrogen bonds, as well as the identity of interacting residues, was recorded. Hydrophobic and *van der Waals* contacts were assessed qualitatively by examining aromatic stacking, alkyl-π interactions, and close approaches between nonpolar atoms. Particular attention was paid to the location and shape of the binding pocket used by each ligand, the balance of binding strength between ATXN3 and LC3 for the same ligand, and the presence of compact, well-packed poses versus more extended and solvent-exposed arrangements. This analysis allowed the ligands to be classified as potential dual target binders or as primarily LC3-biased molecules.

Pharmacokinetic profiling: Pharmacokinetic and drug likeness properties were assessed for all five natural ligands using SwissADME [45]. For each ligand, the following descriptors were calculated: Molecular weight, hydrogen bond donors, acceptors, topological polar surface area (TPSA), consensus logP (lipophilicity), gastrointestinal (GI) absorption prediction, blood-brain barrier permeability, P-glycoprotein substrate status, Lipinski's rule of five violations [46], and bioavailability score. These properties were used to assess oral drug-likeness and to compare the flavonoids with the glycosylated compounds.

Results

Docking energies: Docking data showed that three flavonoids, quercetin, kaempferol, and luteolin [37-39], bound strongly to ATXN3 and LC3, with predicted binding energies around -8 kcal/mol on each target. Rutin and trehalose [40, 41] displayed weaker binding to ATXN3 but strong or good binding to LC3. A side-by-side comparison of predicted docking energies for ATXN3 vs LC3 (AutoDock Vina, kcal/mol) is shown in **Table 2**.

Table 2: ATXN3 versus LC3 docking energies (Vina, kcal/mol)

Ligand	ATXN3 ΔG (kcal/mol)	LC3 ΔG (kcal/mol)	Comment
Quercetin	-8.5	-8.3	Strong on both targets (best dual binder)
Kaempferol	-8.2	-8.3	Strong on both targets
Luteolin	-8.1	-8.4	Strong on both targets
Rutin	-6.4	-10.3	Medium on ATXN3, very strong on LC3
Trehalose	-5.2	-7.8	Weakest on ATXN3, decent on LC3

In the context of AutoDock Vina [36] scoring, binding energies around -8 kcal/mol generally indicate strong predicted affinity, values around -6 kcal/mol indicate moderate affinity, and values closer to -5 kcal/mol suggest relatively weaker but still detectable binding.

Binding to the ATXN3 Josephin domain: All five natural ligands docked to a surface cleft on the ATXN3 Josephin domain defined by residues Gly25-Gly29, Leu26, Ala27, Ala16, Ala45, and Ser114. Quercetin and kaempferol

formed between six and seven hydrogen bonds with backbone and side chain atoms in this region, while at the same time engaging Ala16 and Ala45 through hydrophobic contacts. Their planar aromatic systems fitted snugly into the cleft, producing compact, well packed poses consistent with their strong binding energies (about -8.5 and -8.2 kcal/mol). Luteolin adopted a similar orientation but formed fewer direct hydrogen bonds, relying more on shape complementarity and hydrophobic packing. Despite this, its binding energy remained strongly favorable (about -8.1 kcal/mol), suggesting that precise positioning in the pocket compensates for the smaller hydrogen-bonding network. Rutin and trehalose displayed more extended and solvent-exposed orientations. Rutin formed numerous hydrogen bonds through its sugar moieties but did not fully occupy the central hydrophobic pocket, which may explain its more moderate energy (about -6.4 kcal/mol). Trehalose formed several hydrogen bonds with residues such as Leu23, Leu26, Ser114, Gly29, Ala27, Lys17, and Ala30, but its small, highly polar structure interacted mainly with surface residues and did not pack deeply into the cleft, resulting in the weakest ATXN3 binding among the panel (about -5.2 kcal/mol).The predicted binding orientation of the top ATXN3 binder (quercetin) within the Josephin-domain cleft is shown in **Figure 3**.

Binding to LC3: On LC3, all natural ligands achieved favorable docking scores. Rutin produced the most negative predicted binding energy (about -10.3 kcal/mol). Its bulky glycosidic structure formed a dense network of hydrogen bonds, about ten to eleven, including intra-ligand interactions with residues such as Ser2050, Ala2102, Arg2154, Thr2157, Asn2048, Phe2103, and Gln2127. These interactions spanned multiple polar and charged pockets on the LC3 surface. Quercetin, kaempferol, and luteolin showed strong LC3 binding energies (about -8.4 to -8.3 kcal/mol). Their binding modes involved combinations of polar interactions with residues including Lys2046, Asp2233, Gln1188, Asn2048, and Ser2050, together with aromatic stacking against residues such as Phe1103. Luteolin formed around seven hydrogen bonds (one intra-ligand), whereas quercetin and kaempferol formed fewer hydrogen bonds but benefitted from favorable aromatic packing and *van der Waals* contacts. Trehalose showed a docking energy of about -7.8 kcal/mol on LC3. It formed about seven hydrogen bonds with residues including Lys2046, Asn2048, Gln2127, Asp2081, Asp2045, and His2083. As with its ATXN3 binding, interactions were predominantly polar, with limited hydrophobic packing. A representative LC3-bound pose (kaempferol) illustrating occupancy of the LC3 ligand-binding pocket and the key polar/aromatic contacts is shown in **Figure 4**.

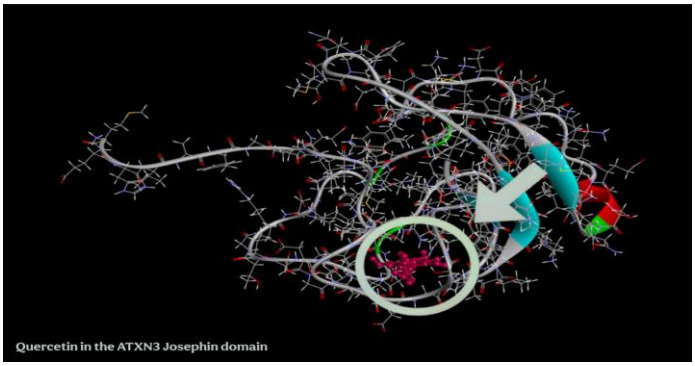

Figure 3: Predicted binding poses of quercetin in the ATXN3 Josephin domain

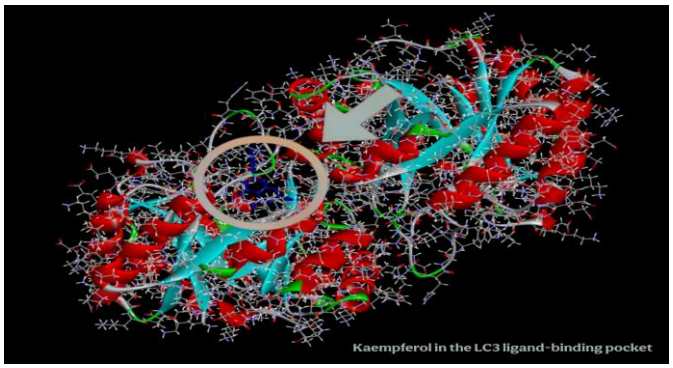

Figure 4: Predicted binding pose of kaempferol in the LC3 ligand-binding pocket

Dual-target versus LC3-biased profiles: Considering ATXN3 and LC3 together, quercetin, kaempferol, and luteolin emerge as dual-target leads. Each display strong and relatively balanced predicted affinities for both proteins, with reproducible binding poses and clear engagement of structurally defined pockets. These features are consistent with the idea that such molecules might, in principle, associate with mutant ATXN3 and LC3 in the same cellular environment and could contribute to an ATTEC-like bridging mechanism. Rutin and trehalose,

by contrast, show LC3-biased behavior. They bind LC3 very strongly, but interact with ATXN3 weakly and in a more superficial manner. This pattern reflects the high polarity introduced by glycosylation, which favors occupancy of the polar grooves on LC3 while reducing compatibility with the shallower, partly hydrophobic ATXN3 cleft. Based on these dual-target versus LC3-biased profiles, a mechanistic hypothesis for an ATTEC-like bridging interaction is illustrated in **Figure 5**.

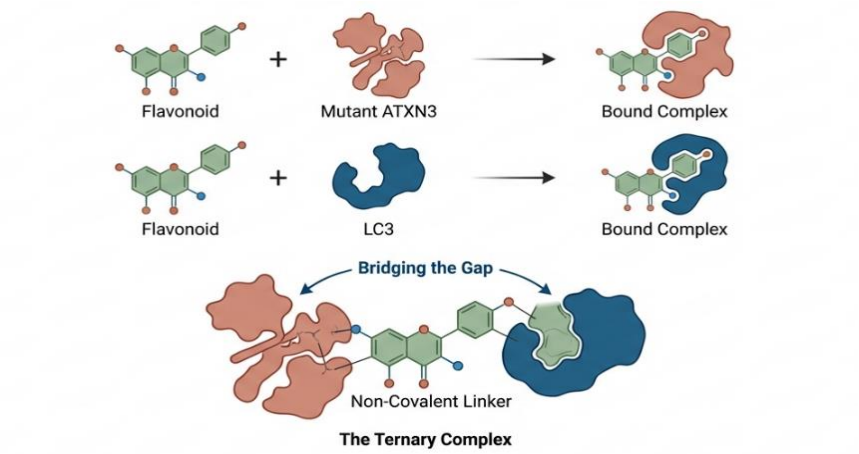

Figure 5: Hypothesized ATTEC-like mechanism of selective autophagy by natural flavonoids

Pharmacokinetic profiling of natural ligands: SwissADME [45] analysis was performed for all five natural ligands to obtain a preliminary assessment of drug likeness and pharmacokinetic suitability. The main descriptors are summarized in **Table 3**.

Table 3: Predicted pharmacokinetic properties of natural ligands obtained from SwissADME

Ligand	MW (g/mol)	HBD	HBA	Rot. bonds	TPSA (Å²)	LogP	GI absorption	Lipinski violations
Quercetin	302.24	5	7	1	131.36	1.23	High	0
Kaempferol	286.24	4	6	1	111.13	1.77	High	0
Luteolin	286.24	4	6	1	111.13	1.73	High	0
Rutin	610.52	10	16	6	269.43	-0.33	Low	3
Trehalose	342.30	8	11	4	189.53	-3.47	Low	2

The three aglycone flavonoids, quercetin, kaempferol, and luteolin, showed molecular weights below 310 g/mol, acceptable lipophilicity (consensus logP 1.23-1.77), and moderate polar surface areas (TPSA 111-131 Å²), with no violations of Lipinski's criteria [46] and predicted high gastrointestinal absorption. Quercetin showed a slightly elevated TPSA (131.36 Å²) due to its extra hydroxyl group, but remained within acceptable limits. All three displayed bioavailability scores of 0.55 and shared a single catechol-related PAINS/Brenk alert, indicating potential for assay interference that would warrant experimental validation. In marked contrast, rutin and trehalose exhibited much more restrictive pharmacokinetic profiles. Rutin had a high molecular weight (610.52 g/mol), very large polar surface area (269.43 Å²), and notably negative lipophilicity (logP -0.33), coupled with low predicted GI absorption, P-glycoprotein substrate status, and three Lipinski rule violations, resulting in a very low bioavailability score of 0.17. Trehalose displayed an even more extreme polar profile, with eight hydrogen bond donors, 11 acceptors, and an exceptionally high TPSA (189.53 Å²) and strongly negative consensus logP (-3.47). It also showed low GI absorption, active P-gp efflux, multiple drug likeness violations, and a minimal bioavailability score of 0.17, indicating that formulation or alternative delivery approaches would be necessary to achieve systemic exposure. These findings underscore a critical distinction: the aglycone flavonoids combine

strong dual target docking with favorable oral druglike properties suitable for immediate translational development, whereas the glycosylated compounds, despite their exceptional LC3 binding, present substantial bioavailability barriers that would require additional pharmaceutical innovation to overcome.

Discussion

The current docking study provides a first exploration of whether common natural compounds can function as dual binders of mutant ATXN3 and LC3. The strong and balanced affinities of quercetin, kaempferol, and luteolin for both targets suggest that such compounds may satisfy the basic structural requirements for ATTEC-like activity [47], namely the ability to associate with the disease protein and with LC3 simultaneously or sequentially. Although docking does not address whether a single molecule can physically bridge two proteins at once, it does indicate that these flavonoids possess complementary interaction surfaces for both partners. In a cellular context, if a flavonoid strongly binds regions exposed on ATXN3 aggregates while displaying high affinity for LC3, it could increase the probability that LC3-decorated autophagosomal membranes form in proximity to ATXN3 aggregates. Such a scenario would tend to favor encapsulation of aggregates within autophagosomes and their subsequent degradation in lysosomes, thereby reducing the burden of toxic ATXN3 species. This conceptual mechanism parallels that proposed for synthetic ATTECs, but relies on simpler, naturally occurring scaffolds. Notably, the SwissADM E [45] profiling reveals that the three flavonoid dual target binders also possess favorable oral drug like properties, molecular weights 286-302 g/mol, high predicted GI absorption, and zero Lipinski violations, supporting their potential for direct therapeutic development without major structural optimization. The catechol PAINS alerts warrant attention [48], as catechol moieties can be reactive in some assays, but their presence in quercetin and kaempferol does not preclude biological activity in cell-based validation studies.

Trehalose has been reported to enhance autophagy and reduce aggregation of polyglutamine proteins, including ATXN3, in experimental models. However, the present results indicate that trehalose interacts rather weakly and superficially with the ATXN3 Josephin domain, while binding LC3 more strongly. This pattern is consistent with the idea that trehalose acts primarily as a global enhancer of autophagy and as a chemical chaperone, rather than as a specific molecular bridge between ATXN3 and LC3. It's very poor oral bioavailability (bioavailability score 0.17, low GI absorption, P--p substrate) further reinforces that its previously reported in vivo effects likely depend on specialized delivery or on local action in specialized compartments rather than systemic exposure. Rutin shows a similar LC3 biased profile, with extremely strong LC3 binding (-10.3 kcal/mol) but moderate ATXN3 affinity (-6.4 kcal/mol). Glycosylation thus appears to enhance LC3 engagement through increased polar interactions, while the large molecular weight and high TPSA simultaneously compromise the compact hydrophobic packing that supports strong ATXN3 binding and severely limit oral absorption (bioavailability score 0.17, low GI absorption).

Docking provides approximate scores and static poses under simplified conditions. Actual binding in cells will depend on factors such as protein dynamics, competition with endogenous ligands, compound solubility, metabolic stability, and cell permeability. Moreover, the Josephin domain alone does not capture the full structural context of the polyglutamine tract and flanking regions of ATXN3, which may contribute additional binding surfaces *in vivo*. Even if dual binding is confirmed biochemically, demonstration of a true ATTEC-like mechanism will require evidence that these compounds increase co-localization of ATXN3 and LC3 and enhance autophagic flux toward ATXN3 in cellular or animal models. Further study should focus on validating the predicted interactions experimentally. Surface plasmon resonance or isothermal titration calorimetry could be used to measure binding affinities of quercetin, kaempferol, and luteolin for purified ATXN3 and LC3 [49]. In parallel, cell-based studies in SCA3 models could test whether these compounds reduce ATXN3 aggregation,

alter LC3-II levels, and promote co-localization of ATXN3 with autophagosomes and lysosomes. Structure-activity relationship studies may optimize dual binding by adjusting hydroxylation patterns or adding linkers that better accommodate the spatial arrangement of the ATXN3 and LC3 binding sites. Given the favorable oral drug-like properties of the aglycone flavonoids, pharmacokinetic studies *in vivo* would be warranted to confirm systemic exposure and target engagement.

Conclusion: Using a Vina-based docking protocol and SwissADME pharmacokinetic profiling, this study reveals that three flavonoids, quercetin, kaempferol, and luteolin, bind strongly and consistently to the ATXN3 Josephin domain and LC3, while simultaneously possessing favorable oral drug-like properties (MW 286-302 g/mol, high GI absorption, zero Lipinski violations, bioavailability scores 0.55). Rutin and trehalose display LC3-biased binding profiles with very poor oral bioavailability characteristics. These findings suggest that natural aglycone flavonoids can provide accessible, drug-like scaffolds for the development of small molecules aimed at promoting selective autophagic clearance of mutant ATXN3 in SCA3.

References

1. Paulson H, Shakkottai V. Spinocerebellar ataxia type 3, GeneReviews. Bookshelf ID: NBK1196, PMID: 20301375.
2. Nagao KJ, Patel N. Spinocerebellar ataxia type 3 | MedLink Neurology. Accessed: Jan. 29, 2026: https://www.medlink.com/articles/spinocerebellar-ataxia-type-3.
3. Machado-Joseph Disease (Spinocerebellar Ataxia Type 3) - Physiopedia. Accessed: Jan. 29, 2026: https://www.physio-pedia.com/Machado-Joseph_Disease_(Spinocerebellar_Ataxia_Type_3).
4. Lima M, Raposo M, Ferreira A, Melo ARV, Pavão S, Medeiros F, et al. The homogeneous Azorean Machado-Joseph disease cohort: Characterization and contributions to advances in research. Biomedicines. 2023; 11(2): 247. doi: 10.3390/biomedicines11020247
5. D'Abreu A, França MC Jr, Paulson HL, Lopes-Cendes I. Caring for Machado-Joseph disease: Current understanding and how to help patients. Parkinsonism and Related Disorders. 2010; 16(1): 2-7. doi: 10.1016/j.parkreldis.2009.08.012
6. Spinocerebellar Ataxias including Machado-Joseph Disease | National Institute of Neurological Disorders and Stroke. Accessed Jan. 29, 2026: https://www.ninds.nih.gov/health-information/disorders/spinocerebellar-ataxias-including-machado-joseph-disease
7. Matos CA, de Almeida LP, Nóbrega C. Machado-Joseph disease/spinocerebellar ataxia type 3: Lessons from disease pathogenesis and clues into therapy. Journal of Neurochemistry. 2019; (1): 8-28. doi: 10.1111/jnc.14541
8. Ross CA, Poirier MA. Protein aggregation and neurodegenerative disease. Nature Medicine. 2004; 10(7): S10-S17. doi: 10.1038/nm1066
9. Mizushima N, Levine B. Autophagy in mammalian development and differentiation. Nature Cell Biology. 2010; 12(9): 823-830. doi: 10.1038/ncb0910-823
10. Kawai Y, Takeda A, Abe Y, Washimi Y, Tanafea F, Sobue G. Cognitive impairments in Machado-Joseph disease. Archives of Neurology. 2004; 61(11): 1757-1760. doi: 10.1001/archneur.61.11.1757
11. Bettencourt C, Lima M. Machado-Joseph disease: From first descriptions to new perspectives. Orphanet Journal of Rare Diseases. 2011; 6(1): 35. doi: 10.1186/1750-1172-6-35
12. Kabeya Y, Mizushima N, Yamamoto A, Oshitani-Okamoto S, Ohsumi Y, Yoshimori T. LC3, GABARAP and GATE16 localize to autophagosomal membrane depending on form-II formation. Journal of Cell Science. 2004; 117(Pt 13): 2805-2812. doi: 10.1242/jcs.01131
13. Delorme-Axford E, Klionsky DJ. The LC3-conjugation machinery specifies cargo loading and secretion of extracellular vesicles. Autophagy. 2020; 16(7): 1169. doi: 10.1080/15548627.2020.1760057
14. Song T, Su H, Yin W, Wang L, Huang R. Acetylation modulates LC3 stability and cargo recognition. FEBS Letters. 2019; 593(4): 414-422. doi: 10.1002/1873-3468.13327
15. Ding Y, Xing D, Fei Y, Luo S, Lu B. Perspectives of autophagy-tethering compounds (ATTECs) in drug discovery. Medicine Plus. 2024; 1(1): 100004. doi: 10.1016/j.medp.2023.100004
16. Li Z, Zhu C, Ding Y, Fei Y, Lu B. ATTEC: A potential new approach to target proteinopathies. Autophagy. 2020; 16(1): 185-187. doi: 10.1080/15548627.2019.1688556

17. Li Z, Wang C, Wang Z, Zhu C, Li J, Sha T, et al. Allele-selective lowering of mutant HTT protein by HTT-LC3 linker compounds. Nature. 2019; 575(7781): 203-209. doi: 10.1038/s41586-019-1722-1
18. Al-Khayri JM, Sahana GR, Nagella P, Joseph BV, Alessa FM, Al-Mssallem MQ. Flavonoids as potential anti-inflammatory molecules: A review. Molecules. 2022; 27(9): 2901. doi: 10.3390/molecules27092901
19. Devi S, Kumar V, Singh K, Dubey k, Kim J. Flavonoids: Potential candidates for the treatment of neurodegenerative disorders. Biomedicines. 2021; 9(2): 1-22. doi: 10.3390/biomedicines9020099
20. Chandrasekaran V, Hediyal TA, Anand N, Kendaganna PH, Gorantla VR, Mahalakshmi AM, et al. Polyphenols, autophagy and neurodegenerative diseases: A review. Biomolecules. 2023; 13(8): 1196. doi: 10.3390/biom 13081196
21. Sarkar S, Davies JE, Huang Z, Tunnacliffe A, Rubinsztein DC. Trehalose, a novel mTOR-independent autophagy enhancer, accelerates the clearance of mutant huntingtin and α-synuclein. Journal of Biological Chemistry. 2007; 282(8): 5641-5652. doi: 10.1074/jbc.M609532200
22. Wang Z, Wang M, Huang Y, Ma Z, Gao W, Zhang T, et al. Trehalose prevents the formation of aggregates of mutant ataxin-3 and reduces soluble ataxin-3 protein levels in an SCA3 cell model. Neuroscience. 2024; 555: 76-82. doi: 10.1016/j.neuroscience. 2024.06.036
23. Tanaka M, Machida Y, Niu S, Ikeda T, Jana NR, Doi H, et al. Trehalose alleviates polyglutamine-mediated pathology in a mouse model of Huntington disease. Nature Medicine. 2004 10(2):148-154. doi: 10.1038/nm985
24. Lin TH, Chen WL, Hsu SF, Chen IC, Lin CH, Chang KH, et al. Small molecules inducing autophagic degradation of expanded polyglutamine protein through interaction with both mutant ATXN3 and LC3. International Journal of Molecular Sciences. 2024; 25(19): 10707. doi: 10.3390/ijms251910707
25. Chen IC, Chen WL, Chang KH, Lee JW, Lin TH, Lin W, et al. Investigating the therapeutic effects of novel compounds targeting inflammatory IL-1β and IL-6 signaling pathways in spinocerebellar ataxia type 3. European Journal of Pharmacology. 2024; 967: 176370. doi: 10.1016/ j.ejphar.2024.176370
26. Procházková D, Boušová I, Wilhelmová N, Antioxidant and prooxidant properties of flavonoids. Fitoterapia. 2011; 82(4): 513-523. doi: 10.1016/j.fitote.2011.01.018
27. Zhang Y, Chen AY, Li M, Chen C, Yao Q. Ginkgo biloba extract kaempferol inhibits cell proliferation and induces apoptosis in pancreatic cancer cells. Journal of Surgical Research. 2008; 148(1): 17-23. doi: 10.1016/j.jss.2008
28. Chandrasekaran V, Hediyal T, Anand N, Kendaganna P, Gorantla V, Mahalakshmi A, et al. Polyphenols, autophagy and neurodegenerative diseases: A review. Biomolecules. 2023; 13(8): 1196. doi: 10.3390/biom13081196
29. Bresciani A, Spiezia MC, Boggio R, Cariulo C, Nordheim A, Altobelli R, Kuhlbrodt K. Quantifying autophagy using novel LC3B and p62 TR-FRET assays. PLoS One. 2018; 13(3): e0194423. doi: 10.1371/journal.pone. 0194423
30. Nicastro G, Menon RP, Masino L, Knowles PP, McDonald NQ, Pastore A. The solution structure of the Josephin domain of ataxin-3: Structural determinants for molecular recognition. Proceedings of the National Academy of Sciences. 2005; 102(30): 10493-10498. doi: 10.1073/pnas.0501732102
31. Mao Y, Senic-Matuglia F, Di Fiore PP, Polo S, Hodsdon ME, De Camilli M. Deubiquitinating function of ataxin-3: insights from the solution structure of the Josephin domain. Proceedings of the National Academy of Sciences. 2005; 102(36): 12700-12705. doi: 10.1073/pnas.0506344102
32. Kabeya Y, Mizushima N, Yamamoto A, Oshitani-Okamoto S, Ohsumi Y, Yoshimori T. LC3, GABARAP and GATE16 localize to autophagosomal membrane depending on form-II formation. Journal of Cell Science. 2004; 117(Pt 13): 2805-2812. doi: 10.1242/JCS.01131
33. Saito K, Arakawa M, Maeda K, Morita E. Autophagosome marker, LC3, is released extracellularly via several distinct pathways. FEBS Open Bio. 2025; 16(3): 542-560. doi: 10.1002/2211-5463.70150
34. Ichimura Y, Kumanomidou T, Sou Y, Mizushima T, Ezaki J, Ueno T, et al. Crystal structure of LC3-p62 complex. Worldwide Protein Data Bank. 2008. doi: 10.2210/pdb2zjd/pdb
35. Protein Data Bank - an overview | ScienceDirect Topics. Accessed: Dec. 24, 2024: https://www.sciencedirect.com /topics/biochemistry-genetics-and-molecular-biology/protein-data-bank
36. Trott O, Olson AJ. AutoDock Vina: Improving the speed and accuracy of docking with a new scoring function, efficient optimization, and multithreading. Journal of Computational Chemistry. 2010; 31(2): 455-461. doi: 10.1002 /JCC.21334
37. Luteolin | C15H10O6 | CID 5280445 - PubChem. Accessed: Jan. 29, 2026: https://pubchem.ncbi.nlm.nih.gov/ compound/Luteolin#section=InChIKey
38. Quercetin | C15H10O7 | CID 5280343 - PubChem. Accessed: Jan. 29, 2026: https://pubchem.ncbi.nlm.nih.gov /compound/5280343

39. Kaempferol | C15H10O6 | CID 5280863 - PubChem. Accessed: Jan. 29, 2026: https://pubchem.ncbi.nlm.nih.gov/compound/Kaempferol#section=InChI
40. Rutin | C27H30O16 | CID 5280805 - PubChem. Accessed: Jan. 29, 2026: https://pubchem.ncbi.nlm.nih.gov/compound/Rutin
41. Trehalose | C12H22O11 | CID 7427 - PubChem. Accessed: Jan. 29, 2026: https://pubchem.ncbi.nlm.nih.gov/compound/Trehalose
42. Inc. (ACD/Labs) Advanced Chemistry Development, ChemSketch [Computer software], 1998, Advanced Chemistry Development, Inc. Accessed: Aug. 14, 2025: https://www.acdlabs.com/products/chemsketch/
43. PyRx - Python Prescription - Virtual Screening Tool. Accessed: Dec. 24, 2024: https://pyrx.sourceforge.io/
44. BIOVIA Discovery Studio Visualizer | Dassault Systèmes. Accessed: Dec. 24, 2024: https://www.3ds.com/products/biovia/discovery-studio/visualization
45. Daina A, Michielin O, Zoete V. SwissADME: A free web tool to evaluate pharmacokinetics, drug-likeness and medicinal chemistry friendliness of small molecules. Scientific Reports. 2017; 7: 42717. doi: 10.1038/srep42717
46. Lipinski CA, Lombardo F, Dominy BW, Feeney PJ. Experimental and computational approaches to estimate solubility and permeability in drug discovery and development settings. Advanced Drug Delivery Reviews. 2001; 46(1-3): 3-26. doi: 10.1016/S0169-409X(00)00129-0
47. Zhao L, Zhao J, Zhong K, Tong A, Jia D. Targeted protein degradation: Mechanisms, strategies and application. Signal Transduction and Targeted Therapy. 2022; 7(1): 113. doi: 10.1038/s41392-022-00966-4
48. Dahlin JL, Nissink JW, Strasser JM, Francis S, Higgins L, Zhou H, et al. PAINS in the assay: Chemical mechanisms of assay interference and promiscuous enzymatic inhibition observed during a sulfhydryl-scavenging HTS. Journal of Medicinal Chemistry. 2015; 58(5): 2091-2113. doi: 10.1021/jm5019093
49. Cuyverset S, Dornez E, Abou Hachem M, Svensson B, Hothorn M, Chory J, et al. Isothermal titration calorimetry and surface plasmon resonance allow quantifying substrate binding to different binding sites of Bacillus subtilis xylanase. Analytical Biochemistry. 2012; 420(1): 90-92. doi: 10.1016 /j.ab.2011.09.005

Author contribution: AMG conceived, designed the study. SHA collected data. SHA, HAG, MAG & AH contributed to data analysis. SHA, AH & AMG performed and interpreted the analysis. SHA & AMG drafted the manuscript. All authors agreed to be accountable for its contents.
Conflict of interest: The authors declare the absence of any commercial or financial relationships that could be construed as a potential conflict of interest.
Ethical issues: The authors completely observed ethical issues, including plagiarism, informed consent, data fabrication or falsification, and double publication or submission.
Data availability statement: The raw data that support the findings of this article are available from the corresponding author upon reasonable request.
Author declarations: The authors confirm that they have followed all relevant ethical guidelines and obtained any necessary IRB and/or ethics committee approvals.
Generative AI disclosure: No generative AI was used in the preparation of this manuscript.